

Cosmic-ray and gamma-ray constraints on very-heavy dark matter decay

Saikat Das,^{a,*} Kohta Murase^{b,c,a} and Toshihiro Fujii^{d,e}

^aCenter for Gravitational Physics and Quantum Information, Yukawa Institute for Theoretical Physics, Kyoto University, Kyoto 606-8502, Japan

^bDepartment of Physics; Department of Astronomy & Astrophysics; Center for Multimessenger Astrophysics, Institute for Gravitation and the Cosmos, The Pennsylvania State University, University Park, Pennsylvania 16802, USA

^cSchool of Natural Sciences, Institute for Advanced Study, Princeton, New Jersey 08540, USA

^dGraduate School of Science, Osaka Metropolitan University, Osaka 558-8585, Japan

^eNambu Yoichiro Institute of Theoretical and Experimental Physics, Osaka Metropolitan University, Osaka 558-8585, Japan

E-mail: saikat.das@yukawa.kyoto-u.ac.jp, murase@psu.edu, toshi@omu.ac.jp

Decaying very-heavy dark matter (VHDM) particles at energies $\gtrsim 10^9$ GeV can contribute to the ultrahigh-energy cosmic ray spectrum. However, the composition measurements by Pierre Auger Observatory indicate the presence of heavy-nuclei dominance at the highest energies. We constrain the flux of $p + \bar{p}$ from Galactic and extragalactic VHDM using the latest spectrum and composition data and incorporating an astrophysical component. This provides improved limits on the VHDM decay timescale at $\lesssim 10^{12}$ GeV. We also calculate the flux of UHE photons from VHDM decay and find that the constraints obtained using integral γ -ray flux upper limits from Auger are more stringent by a factor of ~ 10 . This improves our limits to VHDM lifetime by a factor of two compared to earlier studies.

38th International Cosmic Ray Conference (ICRC2023)
26 July - 3 August, 2023
Nagoya, Japan



*Speaker

1. Introduction

The ‘‘cutoff’’ in the ultrahigh-energy cosmic ray spectrum can arise from the maximum acceleration energy inside astrophysical sources or due to interactions with the cosmic background photons during the propagation. Using the spectrum and composition data from Pierre Auger Observatory and Telescope Array Collaboration [1–5], it is possible to model the injection properties of UHECR sources and their extragalactic propagation [e.g., 6–11]. The hybrid detection technique for extensive air showers, involving fluorescence detectors in addition to the surface detectors, enables precise measurement of the energy and arrival direction of the UHECRs [12, 13].

Different hadronic interaction models lead to a different interpretation of the composition at highest energies. However, a general conclusion is that the composition becomes progressively heavier with increasing energy above $\approx 10^{18.2}$ eV [13–16]. Several candidate source classes for UHECR origin have been proposed and studied, viz., tidal disruption events, gamma-ray bursts, active galactic nuclei, starburst galaxies, and compact object mergers are some of the prominent candidates studied in the literature [e.g., 17, 18]. In addition to the astrophysical sources, they can also originate in the decay or annihilation of dark matter (DM), with a mass up to the grand unification energy $\Lambda_{\text{GUT}} \sim 10^{15} - 10^{16}$ GeV. This may provide a sizeable flux of cosmic rays within the observed energy range.

Multimessenger experiments detecting cosmic rays, neutrinos, and gamma rays can be used for the indirect detection of dark matter decay. The final state Standard Model (SM) particles eventually lead to $p, \bar{p}, \gamma, e^\pm, \nu,$ and $\bar{\nu}$, which can be probed with current and upcoming second-generation telescopes. Extragalactic γ -rays beyond 10^{15} eV undergo electromagnetic cascades and are thus attenuated or absorbed before reaching the earth. Multimessenger constraints on DM decay (or annihilation) have been studied earlier in great detail [19–26].

Here we present improved constraints in the mass range from $10^9 - 10^{15}$ GeV $\lesssim m_\chi \lesssim 10^{15}$ GeV and their contribution to the UHE cosmic rays and γ -rays. We include both Galactic and extragalactic components for the UHE $p + \bar{p}$ fluxes, and an additional astrophysical component with mixed composition, which improves the lower limits on the VHDM decay timescale τ_χ . We use the latest integrated γ -ray flux upper limits from Auger [27–29], for the first time in this work, and provide improved bounds on τ_χ than obtained in earlier studies.

2. UHECRs and UHE gamma rays from VHDM decay

the prompt spectrum of $\chi \rightarrow S + \dots$ is given by the expression

$$\frac{dN_s}{dx} = \frac{1}{\Gamma_0} \frac{d\Gamma}{dx}, \quad (1)$$

where Γ is the inclusive decay rate of χ to S and $\Gamma_0 = 1/\tau_\chi$ is the inverse lifetime of the decay. Here $x = 2E/m_\chi$ is a dimensionless variable. We assume the decay initiates through the process $\chi \rightarrow X\bar{X}$, for an arbitrary standard model particle X , where the particle and antiparticle each carry energy $m_\chi/2$. Finally, X and \bar{X} evolve to produce S , which carries a fraction x of the initial energy.

We use the numerical code HDMSPECTRA [31] to calculate the DM decay spectrum for energies beyond the electroweak symmetry breaking up to the GUT energy scale at $\sim 10^{15} - 10^{16}$ GeV. We

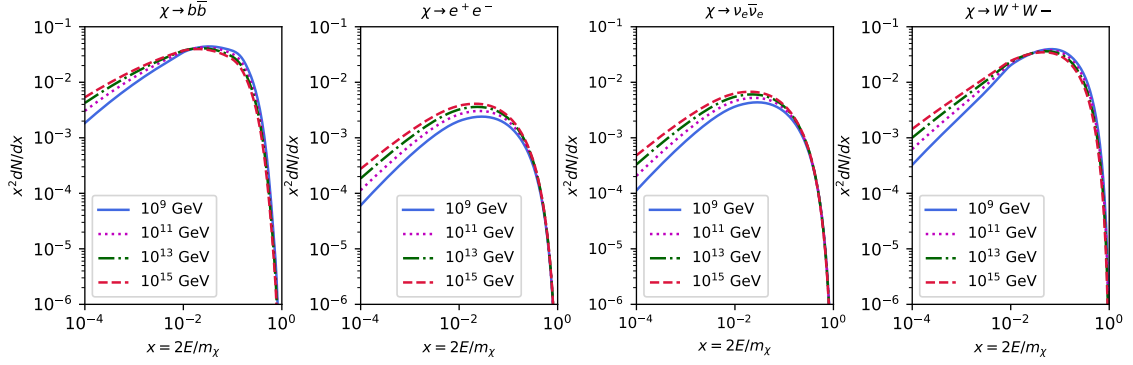


Figure 1: $p + \bar{p}$ prompt spectra from various DM decay modes into Standard Model particles. The different line styles represent the energies $m_\chi = 10^{10}, 10^{13}, 10^{16}, 10^{19}$ GeV as indicated. The figure is reused from Ref. [30].

show the $p + \bar{p}$ fluxes in Fig. 1 for $m_\chi = 10^{15}$ GeV, corresponding to some of the widely considered decay modes in the literature. We use the Navarro-Frenk-White DM density distribution model given as [32],

$$\rho_{\text{NFW}}(R) = \frac{\rho_0}{(R/R_s)^\beta (1 + R/R_s)^{3-\beta}} \quad (2)$$

where $\beta = 1$ and $R_s = 11$ kpc is the scale radius. We take $R_h = 100$ kpc as the size of the Galactic halo and $R_{\text{sc}} = 8.34$ kpc as the distance between the Sun and the Galactic center. The DM density in the solar neighborhood is taken as $\rho_{\text{sc}} c^2 = 0.43$ GeV/cm³ [33], which gives the constant ρ_0 . The boundary of the halo in the angular direction θ is

$$s_{\text{max}}(\theta) = R_{\text{sc}} \cos \theta + \sqrt{R_h^2 - R_{\text{sc}}^2 \sin^2 \theta} \quad (3)$$

The line-of-sight component of the flux of S from direction θ is then,

$$\begin{aligned} \Phi(E, \theta) &= \frac{1}{4\pi m_\chi \tau_\chi} \frac{dN_s}{dE} \int_0^{s_{\text{max}}(\theta)} \rho_\chi(R(s)) ds \\ &= \frac{\rho_{\text{sc}} R_{\text{sc}}}{4\pi m_\chi \tau_\chi} \frac{dN_s}{dE} \mathcal{J}^{\text{dec}}(\theta), \end{aligned} \quad (4)$$

which yields the Galactic contribution of DM decay by performing the following integration up to $\theta = \pi$.

$$\Phi_{\text{G}}(E, \leq \theta) = \frac{\rho_{\text{sc}} R_{\text{sc}}}{4\pi m_\chi \tau_\chi} \frac{dN_s}{dE} \mathcal{J}_\Omega^{\text{dec}} \quad (5)$$

$$\text{where, } \mathcal{J}_\Omega^{\text{dec}} = \frac{2\pi}{\Omega} \int_0^\theta \sin \theta d\theta \mathcal{J}^{\text{dec}}(\theta). \quad (6)$$

Here, $\Omega = 2\pi(1 - \cos \theta)$ is the solid angle of the field of view, and the integration in Eqn. 4 is carried out by changing the variable from line-of-sight coordinate s to Galactocentric distance R .

For the extragalactic case, we assume a uniform DM density distribution in the comoving distance range of 1 Mpc to 5 Gpc. We use the publicly available code CRPROPA 3 to simulate

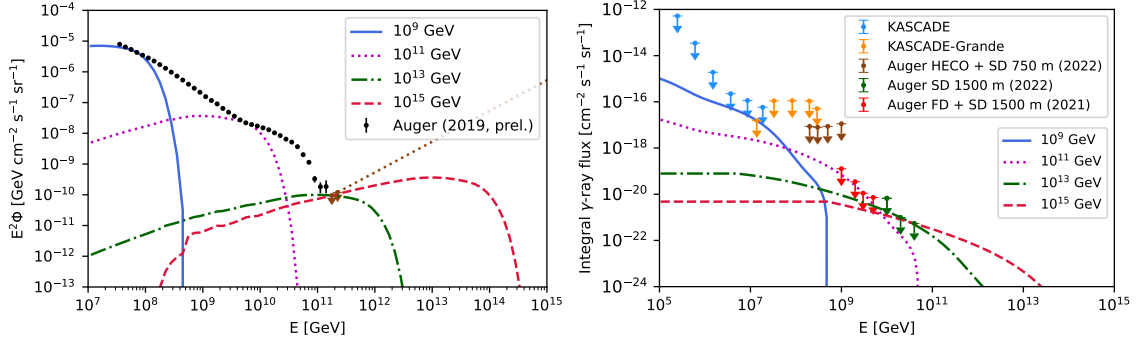


Figure 2: *Left:* $p + \bar{p}$ fluxes at Earth from Galactic + extragalactic DM combined for different values of DM mass $m_\chi = 10^9, 10^{11}, 10^{13},$ and 10^{15} GeV; decaying through the $b\bar{b}$ channel. The black-colored data points are UHECR spectrum data from [35]. The brown-colored upper limits at the highest energy bins are derived using the surface detector data. An extrapolation of the upper limit at higher energies is shown by the dotted line. *Right:* Integrated γ -ray fluxes at Earth from the Galactic DM for discrete values of DM mass $m_\chi = 10^9, 10^{11}, 10^{13},$ and 10^{15} GeV; decaying through $b\bar{b}$ channel. The upper limits on the flux from KASCADE, KASCADE-Grande [36], and Pierre Auger Observatory [27–29] are shown. The KASCADE limits are converted from 90% C.L. to 95% C.L. assuming Poisson statistics. We consider the NFW density profile for DM distribution. The figure is reused from Ref. [30].

the cosmological propagation of cosmic-ray spectrum resulting from prompt DM decay [34]. The cosmic-ray protons undergo various energy loss processes, viz., photomeson production, Bethe-Heitler pair creation, and β -decay of secondary neutrons. In addition, all particles lose energy due to the adiabatic expansion of the universe. The resulting flux can be expressed as

$$\Phi_{\text{EG}}(E) = \frac{c\Omega_\chi\rho_c}{4\pi m_\chi\tau_\chi} \int dz \left| \frac{dt}{dz} \right| F(z) \int dE' \frac{dN'_s}{dE'} \frac{d\eta}{dE}(E, E', z) \quad (7)$$

where dN'_s/dE' is the injection spectrum from prompt decay of DM and $d\eta/dE$ is the fraction of cosmic-ray protons (or antiprotons) produced with energy E from parent particle of energy E' . The redshift evolution of cosmic-ray injection for the DM case is considered to be $F(z) = 1$. Here, ρ_c is the critical density in a flat FRW universe and $\rho_\chi = \Omega_\chi\rho_c$. We take $\Omega_\chi h^2 = 0.113$ and $\rho_c c^2 h^{-2} = 1.05 \times 10^{-5}$ GeV cm $^{-3}$, where h is the dimensionless Hubble constant. $|dt/dz|$ is the cosmological line element.

3. Results

3.1 UHECRs

The hybrid data of cosmic-ray flux measured by Auger, is available up to $\log_{10}(E/\text{eV}) = 20.15$. An analysis considering 100% efficiency of the surface detector above 10^{20} eV can impose 90% C.L. upper limits on the UHECR flux up to $\log_{10}(E/\text{eV}) = 20.35$ [1, 37]. A linear extrapolation of the upper limits in the logarithmic energy scale serves as a constraint for UHECR flux from VHDM decay at these extreme energies. This, in turn, provides a lower bound to the DM decay timescale τ_χ . The flux of the extragalactic component is orders of magnitude lower than the Galactic component due to higher energy losses. The lower limit to τ_χ is found by the condition that the simulated flux

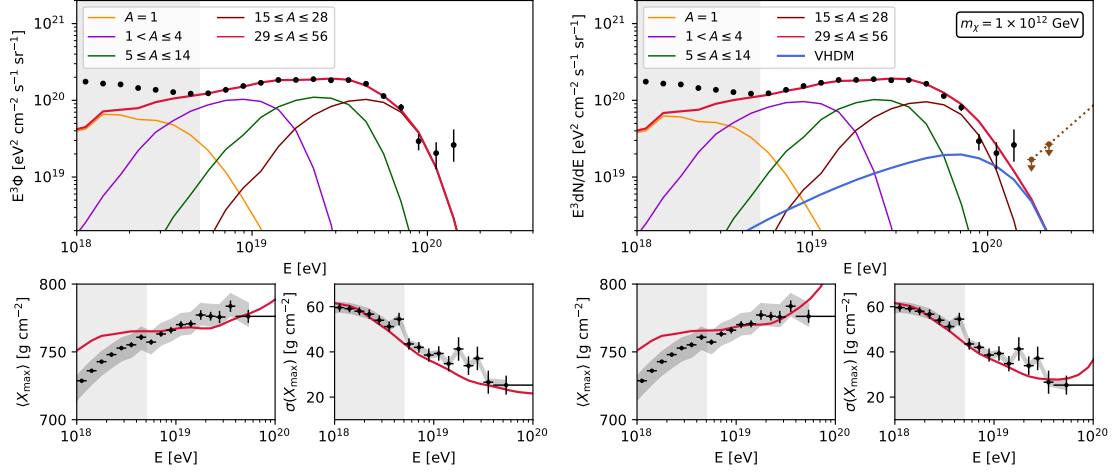


Figure 3: The left panel shows the simulated UHECR spectrum, X_{\max} , and $\sigma(X_{\max})$ for the best-fit source parameters obtained by a combined fit of spectrum and composition with the Auger data. The shaded region is excluded from the fit. Here only astrophysical contribution is assumed from a homogeneous source distribution. The right panel shows the simultaneous contribution from the astrophysical and DM components for $m_\chi = 1 \cdot 10^{12}$ GeV. The fractional contribution from VHDM decay corresponds to 95% C.L. value of χ^2 statistic. See text for more details. The figure is reused from Ref. [30].

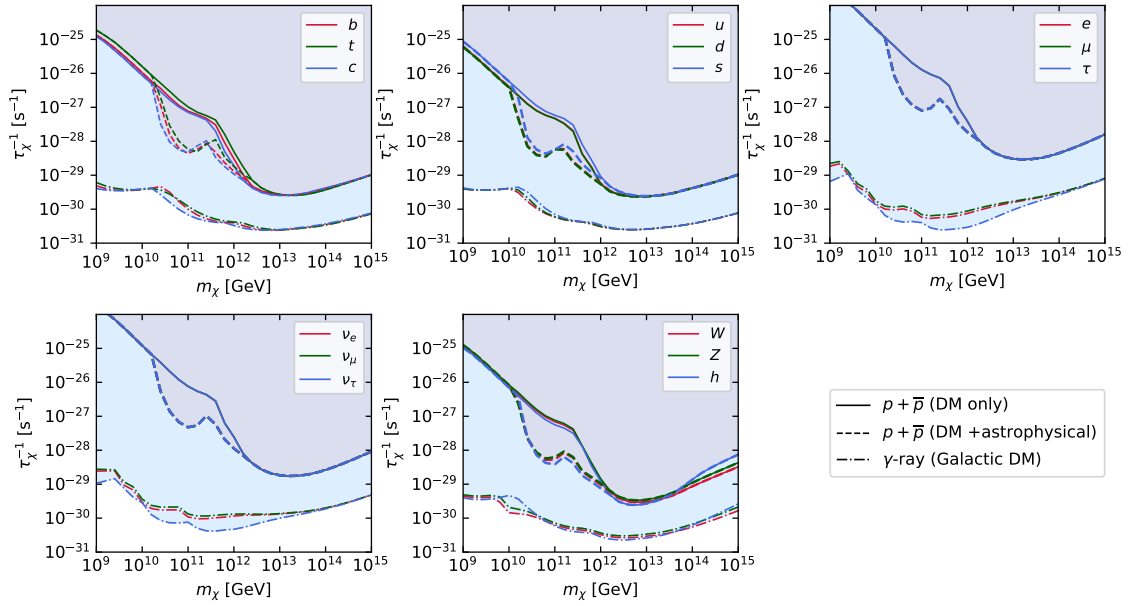


Figure 4: DM decay rate constrained by the observed UHECR flux. The solid line corresponds to $p + \bar{p}$ constraints from only the DM scenario and the dashed line is a more stringent limit when both DM (Galactic + extragalactic) and astrophysical components are considered. A number of initial states from prompt DM decay are considered as indicated in the plot labels. It can be seen that the results obtained for all the leptons e , μ , and τ are identical. The same is applicable to different neutrino flavors and vector bosons. The dashed-dotted lines indicate γ -ray constraints from Galactic DM decay. The figure is reused from Ref. [30]

POS (ICRC2023) 1487

in any energy bin i is $J_i \leq M_i + n \times \Sigma_i$ where M_i is the observed cosmic-ray flux and Σ_i is the error in the i -th energy bin [38]. The values of $n = 1.28, 1.64, 4.3$ corresponds to 90, 95, and 99.9999% C.L. lower limits. The observed $p + \bar{p}$ flux at Earth from DM decay in $\chi \rightarrow b\bar{b}$ channel is shown in the left panel of Fig. 2 for discrete values of m_χ in the range $10^9 \text{ GeV} \leq m_\chi \leq 10^{15} \text{ GeV}$. The fluxes correspond to 95% C.L. lower limit on τ_χ .

Next, we calculate the values of τ_χ when both astrophysical and DM components are present. The best-fit values of the UHECR source parameters are obtained by scanning over the grid of plausible ranges. We assume a mixed composition of representative stable nuclei Hydrogen (^1H), Helium (^4He), Nitrogen (^{14}N), Silicon (^{28}Si), and Iron (^{56}Fe). We use the Gumbel distribution function $g(X_{\text{max}}|E, A)$ to calculate the distribution of the maximum of shower depth $\langle X_{\text{max}} \rangle$ and the shower-to-shower fluctuation $\sigma(X_{\text{max}})$ [39]. The goodness-of-fit is calculated using a χ^2 statistic. See Ref. [30] for more details. For simplicity, we have considered a homogeneous source distribution over redshift. We vary the normalization of the astrophysical component, keeping all other parameters fixed, to add $p + \bar{p}$ fluxes from DM decay, so that $\Phi = A_1 \Phi_\chi + A_2 \Phi_{\text{astro}}$. The 95% C.L. lower limit to τ_χ , in this case, is obtained from the value of A_2 that gives p -value = 0.0455 (32 d.o.f) for the combined χ^2 fit at $E \gtrsim 10^{18.7} \text{ eV}$. A representative case is shown in the right panel of Fig. 3 for $b\bar{b}$ decay mode and $m_\chi = 10^{12} \text{ GeV}$.

3.2 UHE photons

The contribution to γ -ray fluxes from extragalactic dark matter is negligible in our energy range of interest. Also, the mean free path of γ -rays from the prompt DM decay is larger than the Galactic length scales, and hence the cascades can be neglected for the Galactic contribution. At lower energies $E_\gamma < 10^9 \text{ GeV}$, we use the isotropic diffuse γ -ray flux upper limits from KASCADE, KASCADE-Grande [36] and the latest Auger SD upper limits for the first time in this work [27–29], which gives the best up-to-date constraints on the VHDM lifetime at $m_\chi \gtrsim 10^{12} \text{ GeV}$. In the right panel of Fig. 2, we show the integrated γ -ray fluxes from DM decay, constrained by the integrated γ -ray limits. Improvement in the Auger SD limits by $\gtrsim 40\%$ provides tighter bounds than those obtained in earlier studies. Fig. 4 shows the τ_χ^{-1} as a function of m_χ as obtained in this analysis for various channels of DM decay and both cosmic rays and γ -rays. It can be seen the limits imposed by γ -ray constraints are more stringent than that from cosmic rays. The gray-shaded region corresponds to that excluded by both cosmic-ray and γ -ray constraints, while the white region is the allowed range at 95% C.L.

4. Summary

Current γ -ray experiments are sensitive in the GeV-TeV energy band. Imaging atmospheric Cherenkov telescopes, e.g., H.E.S.S., VERITAS, and MAGIC, as well as other air-shower detectors such as HAWC and LHAASO are crucial to probe DM signals from the Galactic center direction [40–42]. In this work, we focus on decaying DM with $10^9 \text{ GeV} \leq m_\chi \leq 10^{15} \text{ GeV}$ using Galactic and cosmological DM decay, constrained by the latest cosmic-ray data and γ -ray flux upper limits obtained from Auger.

The constraints from cosmic rays are improved due to the addition of the astrophysical fluxes. In addition, we take into account the UHECR composition data ($\langle X_{\text{max}} \rangle$ and $\sigma(X_{\text{max}})$), as well as

explore a wide range of lepton, quark, and gauge boson decay modes. The cosmic-ray flux constrains τ_χ to $\gtrsim 4 \times 10^{29}$ s at 10^{13} GeV for the $q\bar{q}$ decay channel. The integrated γ -ray flux upper limits from Auger provide tighter constraints on the DM decay lifetime. We find that the γ -ray flux upper limits constrain the VHDM lifetime to $\tau_\chi \gtrsim 4 \times 10^{30}$ s at 10^{13} GeV for the $b\bar{b}$ channel, which is an order of magnitude longer than the former. Using the latest Auger SD upper limits for the first time in this work and considering all decay modes into Standard Model particles in our study, our results indicate $\tau_\chi \gtrsim 10^{30}$ s for 10^{11} GeV $< m_\chi < 10^{15}$ GeV.

It is possible to calculate the solid angle averaged \mathcal{J} factor (given in Eqn. 6) over the Auger field-of-view. Using the NFW model, this results in $\approx 5\%$ change in the τ_χ estimates, deduced from Galactic γ -ray flux. Again, the uncertainties in the DM profile can lead to uncertainty in the sensitivity of detectors [25]. We find that using the Einasto density profile, the resulting change is less than 5% of the values obtained using the NFW profile.

References

- [1] A. Aab *et al.* (Pierre Auger), *Phys. Rev. D* **102**, 062005 (2020).
- [2] P. Abreu *et al.* (Pierre Auger), *Eur. Phys. J. C* **81**, 966 (2021).
- [3] A. Aab *et al.* (Pierre Auger), *Front. Astron. Space Sci.* **6**, 24 (2019).
- [4] R. Abbasi *et al.*, *PoS ICRC2021*, 305 (2021).
- [5] R. Abbasi *et al.*, *PoS ICRC2021*, 203 (2021).
- [6] A. Aab *et al.* (Pierre Auger), *JCAP* **04**, 038 (2017), [Erratum: *JCAP* 03, E02 (2018)].
- [7] R. Alves Batista, R. M. de Almeida, B. Lago, and K. Kotera, *JCAP* **01**, 002 (2019).
- [8] S. Das, S. Razzaque, and N. Gupta, *Phys. Rev. D* **99**, 083015 (2019).
- [9] J. Heinze, A. Fedynitch, D. Boncioli, and W. Winter, *Astrophys. J.* **873**, 88 (2019).
- [10] S. Das, S. Razzaque, and N. Gupta, *Eur. Phys. J. C* **81**, 59 (2021).
- [11] Y. Jiang, B. T. Zhang, and K. Murase, *Phys. Rev. D* **104**, 043017 (2021).
- [12] R. U. Abbasi *et al.* (Telescope Array), *Astrophys. J.* **858**, 76 (2018).
- [13] A. Aab *et al.* (Pierre Auger), *Phys. Rev. D* **90**, 122005 (2014).
- [14] A. Aab *et al.* (Pierre Auger), *Phys. Rev. D* **90**, 122006 (2014).
- [15] J. Bellido (Pierre Auger), *PoS ICRC2017*, 506 (2018).
- [16] A. Aab *et al.* (Pierre Auger), *JCAP* **03**, 018 (2019).
- [17] P. Mészáros, D. B. Fox, C. Hanna, and K. Murase, *Nature Rev. Phys.* **1**, 585 (2019).
- [18] R. Alves Batista *et al.*, *Front. Astron. Space Sci.* **6**, 23 (2019).

- [19] M. Kachelriess and P. D. Serpico, *Phys. Rev. D* **76**, 063516 (2007).
- [20] H. Yuksel, S. Horiuchi, J. F. Beacom, and S. Ando, *Phys. Rev. D* **76**, 123506 (2007).
- [21] K. Murase and J. F. Beacom, *JCAP* **10**, 043 (2012).
- [22] A. Esmaili, A. Ibarra, and O. L. G. Peres, *JCAP* **11**, 034 (2012).
- [23] K. Murase, R. Laha, S. Ando, and M. Ahlers, *Phys. Rev. Lett.* **115**, 071301 (2015).
- [24] K. Ishiwata, O. Macias, S. Ando, and M. Arimoto, *JCAP* **01**, 003 (2020).
- [25] C. Guépin, R. Aloisio, A. Cummings, L. A. Anchordoqui, J. F. Krizmanic, A. V. Olinto, M. H. Reno, and T. M. Venters, *Phys. Rev. D* **104**, 083002 (2021).
- [26] C. A. Argüelles, D. Delgado, A. Friedlander, A. Kheirandish, I. Safa, A. C. Vincent, and H. White, (2022), [arXiv:2210.01303 \[hep-ph\]](https://arxiv.org/abs/2210.01303) .
- [27] P. Savina (Pierre Auger), *PoS ICRC2021*, 373 (2021).
- [28] P. Abreu *et al.* (Pierre Auger), *Astrophys. J.* **933**, 125 (2022).
- [29] P. Abreu *et al.* (Pierre Auger), (2022), [arXiv:2209.05926 \[astro-ph.HE\]](https://arxiv.org/abs/2209.05926) .
- [30] S. Das, K. Murase, and T. Fujii, *Phys. Rev. D* **107**, 103013 (2023), [arXiv:2302.02993 \[astro-ph.HE\]](https://arxiv.org/abs/2302.02993) .
- [31] C. W. Bauer, N. L. Rodd, and B. R. Webber, *JHEP* **06**, 121 (2021).
- [32] J. F. Navarro, C. S. Frenk, and S. D. M. White, *Astrophys. J.* **490**, 493 (1997).
- [33] E. V. Karukes, M. Benito, F. Iocco, R. Trotta, and A. Geringer-Sameth, *JCAP* **09**, 046 (2019).
- [34] R. Alves Batista, A. Dundovic, M. Erdmann, K.-H. Kampert, D. Kuempel, G. Müller, G. Sigl, A. van Vliet, D. Walz, and T. Winchen, *JCAP* **05**, 038 (2016).
- [35] A. Aab *et al.* (Pierre Auger), *PoS ICRC2021* (2019), [arXiv:1909.09073 \[astro-ph.HE\]](https://arxiv.org/abs/1909.09073) .
- [36] W. D. Apel *et al.* (KASCADE Grande), *Astrophys. J.* **848**, 1 (2017).
- [37] A. Aab *et al.* (Pierre Auger), *Phys. Rev. Lett.* **125**, 121106 (2020).
- [38] A. A. Abdo *et al.* (Fermi-LAT), *JCAP* **04**, 014 (2010), [arXiv:1002.4415 \[astro-ph.CO\]](https://arxiv.org/abs/1002.4415) .
- [39] M. De Domenico, M. Settimo, S. Riggi, and E. Bertin, *J. Cosmol. Astropart. Phys.* **2013**, 050 (2013).
- [40] H. Abdallah *et al.* (H.E.S.S.), *Phys. Rev. Lett.* **117**, 111301 (2016), [arXiv:1607.08142 \[astro-ph.HE\]](https://arxiv.org/abs/1607.08142) .
- [41] A. U. Abeysekara *et al.* (HAWC), *JCAP* **02**, 049 (2018), [arXiv:1710.10288 \[astro-ph.HE\]](https://arxiv.org/abs/1710.10288) .
- [42] M. L. Ahnen *et al.* (MAGIC, Fermi-LAT), *JCAP* **02**, 039 (2016), [arXiv:1601.06590 \[astro-ph.HE\]](https://arxiv.org/abs/1601.06590) .